© The American Society of Gene & Cell Therapy

Ad-HEX-transduced cells exhibit hepatic functions

To test the hepatic function in the Ad-HEX-transduced cells, we investigated the liver metabolism, because P450 cytochrome enzymes play a critical role in this function. We examined the expression level of several members of this multigene family, *i.e.*, *CYP3A4*, *CYP7A1*, mRNA and *CYP2D6* in Ad-HEX-transduced cells by real-time RT-PCR. The real-time RT-PCR analysis showed that the mRNAs for *CYP3A4*, *CYP7A1*, and *CYP2D6* were expressed in Ad-HEX-transduced cells, whereas none of these mRNAs were expressed in the nontransduced cells (**Figure 6a**). The expression levels of *CYP3A4* in Ad-HEX-transduced cells were similar to those observed in primary human hepatocytes, which were cultured 48 hours after plating the cells, or fetal liver tissues but lower than those in adult liver. The *CYP2D6* and *CYP7A1* mRNA expressions in Ad-HEX-transduced cells were lower than those in primary hepatocytes or adult tissues. Next, we investigated the metabolism of the P450 3A4 substrates by measuring the activity of P450 isozymes. The metabolites were detected in Ad-HEX-transduced cells, and their activity was 3.4-fold higher than that in the most commonly used human hepatocyte cell line, HepG2 (**Figure 6b**; DMSO column). This result was consistent with the real-time RT-PCR data (**Figure 6a**). We further tested the induction of CYP3A4 upon chemical stimulation, because CYP3A4 is the most prevalent P450 isozyme in the liver and is involved in the metabolism of a significant proportion of the currently available commercial drugs. Because CYP3A4 can be induced with rifampicin, both Ad-HEX-transduced cells and HepG2 cells were treated with rifampicin, followed by treatment with CYP3A4 substrate. Ad-HEX-transduced cells produced 5.4-fold higher levels of metabolites in response to rifampicin treatment (**Figure 6b**; rifampicin column). This result indicates that P450 isozymes are active in Ad-HEX-transduced cells.

DISCUSSION

The object of this study was to develop an efficient method for generating hepatoblasts and hepatocytes from human ESCs and iPSCs for application to drug toxicity screening tests as well as therapeutics such as regenerative medicine. We found that transient HEX transduction in the definitive endoderm together with a culture under chemically defined conditions was useful for this purpose.

It has been reported that a high concentration of Activin A induces differentiation of human ESCs into the definitive endoderm.[8,33,34] On the other hand, undifferentiated human ESCs are maintained by a low concentration of Activin A.[35] Several studies have shown that bFGF promotes the differentiation of ESCs into the definitive endoderm and inhibits the differentiation of ESCs into the extra-embryonic endoderm.[35–38] bFGF has been reported to inhibit the BMP signaling, which can promote the extra-embryonic lineage differentiation.[39] The extra-embryonic endoderm expresses most of the hepatocyte markers, such as AFP.[40] Contamination of the extra-embryonic endoderm makes it difficult to estimate the hepatic differentiation from human ESCs and iPSCs.[11,14,40] In this study, we showed that both Activin A and bFGF induce definitive endoderm populations, while they repress the extra-embryonic endoderm differentiation (**Figure 2g,h**). Interestingly, after the differentiated cells that were cultured on laminin-coated plates with Activin A and bFGF were passaged at day 5, FOXA2-positive cells (definitive endoderm) were enriched in the resultant cells at day 6 (**Figure 2a–f**). This may have been because FOXA2-positive cells efficiently adhered to the laminin-coated plate and/or because trypsinized, single undifferentiated ESCs/iPSCs cannot survive. The passaging of differentiated cells might be attributed to the reduction in the number of not only the extra-embryonic endoderm cells but also the undifferentiated cells. However, the efficiency of the definitive endoderm differentiation in this study was not as efficient as that reported by other groups.[8,33,34] Other cell lineages, such as the mesoderm and extra-embryonic endoderm, might remain at day 6 (**Figure 2g,h** and **Supplementary Figure S1**). Further improvement of the culture conditions will thus be needed in order to enhance the definitive endoderm differentiation.

Hepatoblasts and hepatocytes were differentiated from the human ESC- and iPSC-derived definitive endoderms by transient overexpression of the homeobox gene *HEX*. A fiber-modified Ad vector containing K7 peptides mediated much higher gene expression than conventional Ad vectors in the human ESC- and iPSC-derived definitive endoderms (**Supplementary Figure S6**). This new hepatic differentiation protocol shows that *HEX* induces AFP-positive hepatoblasts at day 9 and ALB-positive hepatocytes at day 12 from human ESCs and iPSCs, whereas the previous protocols require a few weeks or months to induce AFP- and ALB-positive hepatocytes from PSCs.[9–11] Previous studies suggested that *HEX* could regulate liver-enriched transcription factors such as hepatocyte nuclear factor 4A and hepatocyte nuclear factor 6.[19,23] Overexpression of the *HEX* gene under the conditions employed in the present study could activate several transcription factors that are required for hepatic differentiation (**Supplementary Figure S4a,b**). However, the Ad-HEX-transduced cells showed a low level of expression of *ALB* and some CYP450 species, as well as a high level of *AFP* expression, indicating that the cells were still immature. To promote further hepatic differentiation or maturation, it may be effective to culture the hepatic cells in a 3D environment or on feeder cells such as cardiomyocyte- or endothelium-derived cells.[41,42] In addition, the function of our hepatic cells was still limited. Further analysis of the other functions of our hepatic cells, such as glycogen storage, uptake of indocyanine green and organic anion low-density lipoprotein, and transplantation of Ad-HEX-transduced cells into the liver of immunodeficient mice, is clearly needed for the appreciation to drug screening and therapeutic treatment modalities.

During the preparation of this article, Kubo *et al.* have reported that *HEX* could promote hepatoblast differentiation from mouse ESCs.[43] Their report is consistent with our data, suggesting that *HEX* plays a pivotal regulatory role in not only mouse but also human hepatic differentiation. They also showed that the overexpression of *HEX* at the definitive endoderm stage is critical for hepatic specification of the mouse ESCs. We also confirmed that forced expression of *HEX* in the undifferentiated human ESCs and iPSCs did not elevate the expression of *ALB* and *CK7* (**Supplementary Figure S7**), indicating that *HEX* enhances the hepatic differentiation not from the undifferentiated cells but from the definitive endoderm. However, Kubo *et al.* used recombinant mouse ESCs (tet-HEX ESCs), in which the tetracycline-regulated *HEX* expression cassette

© The American Society of Gene & Cell Therapy

is integrated into the host cell genome to induce *HEX* in a stage-specific manner. Their system would not be appropriate for clinical use because the transgene is randomly integrated into the host cell genome and this leads to a risk of mutagenesis.[44] On the other hand, we generated human hepatoblasts by Ad vector-mediated transient *HEX* transduction, method which avoids the integration of exogenous DNA into the host chromosome.

Touboul *et al.* reported that human ESCs and iPSCs can differentiate into functional hepatocytes under chemically defined conditions.[34] In the present study, hepatoblasts were generated in a chemically defined serum-free medium, which minimized exposure to animal cells and proteins, and on a defined extracellular matrix, such as laminin or collagen, which do not contain undefined growth factors. To generate hepatocytes, hepatocyte culture medium, which is serum-free but not defined, was used in the stage III. When defined hESF-medium was used in the stage III, the expression levels of *ALB* and *CYP3A4* mRNA were half the levels seen in the cells cultured with hepatocyte culture medium in the preliminary experiment (data not shown). Human ESCs and iPSCs were also grown for maintaining the undifferentiated state on a feeder layer, which contains xenoantigen such as bovine apolipoprotein B-100. Bovine apolipoprotein B-100 is known to be a dominant xenoantigen for cell-based therapies.[45] Human ESC- and iPSC-derived hepatocytes should be generated and cultured under chemically defined conditions not only to avoid potential contamination with pathogens for the safer therapeutic application, but also to obtain reproducible results using the differentiation protocols.[34,46] Development of differentiation protocols using other genes of transcription factors as well as *HEX* genes based on a chemically defined medium is under way. Overall, our strategy should provide a novel protocol for hepatic differentiation from human ESCs and iPSCs, which could be useful for regenerative medicine and drug screening.

MATERIALS AND METHODS

Ad vectors. Ad vectors were constructed by an improved *in vitro* ligation method.[47,48] The human *HEX* complementary DNA derived from pDNR-LIB-*HEX* (Invitrogen, Carlsbad, CA) was inserted into pHMEF5,[29] which contains the human elongation factor-1α promoter, resulting in pHMEF-HEX. The pHMEF-HEX was digested with I-CeuI/PI-SceI and ligated into I-CeuI/PI-SceI-digested pAdHM41-K7,[30] resulting in pAd-HEX. Ad-HEX and Ad-LacZ, both of which contain the elongation factor-1α promoter and a stretch of lysine residues (K7) peptides in the C-terminal region of the fiber knob, were generated and purified as described previously.[26,29] The vector particle titer was determined by using a spectrophotometric method.[49]

Human ESCs and iPSCs culture. A human ESC line, khES1, was obtained from Kyoto University (Kyoto, Japan).[50] khES1 was used following the Guidelines for Derivation and Utilization of Human Embryonic Stem Cells of the Ministry of Education, Culture, Sports, Science and Technology of Japan after approval by the review board at Kyoto University. Human ESCs were maintained on a feeder layer of mitomycin-inactivated mouse embryonic fibroblasts (ICR; ReproCELL Incorporated, Tokyo, Japan) with Dulbecco's modified Eagle's medium/F-12 (Sigma, St Louis, MO) supplemented with 0.1 mmol/l 2-mercaptoethanol, 0.1 mmol/l nonessential amino acids, 2 mmol/l L-glutamine, 20% GIBCO knockout serum replacement (Invitrogen), and 5 ng/ml bFGF (Sigma) in a humidified atmosphere of 3% CO_2 and 97% air at 37 °C. Human ESCs were dissociated with 0.1 mg/ml dispase (Roche Diagnostics, Burgess Hill, UK) into small clumps, and subcultured every 5 or 6 days.

Two human iPS clones derived from the embryonic human lung fibroblast cell line MCR5 were provided from JCRB Cell Bank (Tic, JCRB Number: JCRB1331; and Dotcom, JCRB Number: JCRB1327).[3,4] In the present study, we mainly used the Tic cell line, but similar results were obtained using the Dotcom cell line, and these are shown in the supplementary figures. Human iPSCs were maintained on a feeder layer of mitomycin-inactivated mouse embryonic fibroblasts (Hygro Resistant Strain C57/BL6; Hygro, Millipore, MA) on a gelatin-coated flask in human iPS medium. Human iPS medium consists of knockout Dulbecco's modified Eagle's medium/F12 (Invitrogen), supplemented with 0.1 mmol/l 2-mercaptoethanol, 0.1 mmol/l nonessential amino acids, 2 mmol/l L-glutamine, 20% knockout serum replacement, and 10 ng/ml bFGF in a humidified atmosphere of 5% CO_2 and 95% air at 37 °C. Human iPSCs were dissociated with 0.1 mg/ml dispase (Roche) into small clumps and subcultured every 7 or 8 days.

In vitro *differentiation*. Before the initiation of cellular differentiation, the medium of human ESCs and iPSCs was exchanged for a defined serum-free medium hESF9 and cultured in a humidified atmosphere of 10% CO_2 and 90% air at 37 °C.[46] hESF9 consists of hESF-GRO medium (Cell Science & Technology Institute, Sendai, Japan) supplemented with five factors (10 μg/ml human recombinant insulin, 5 μg/ml human apotransferrin, 10 μmol/l 2-mercaptoethanol, 10 μmol/l ethanolamine, 10 μmol/l sodium selenite), oleic acid conjugated with fatty acid free bovine ALB, 10 ng/ml bFGF, and 100 ng/ml heparin (all from Sigma). For induction of definitive endoderm, human ESCs and iPSCs were dissociated into single cells with Accutase (Invitrogen) and cultured for 5 days on a mouse laminin-coated tissue 12-well plate (6.0×10^4 cells/cm^2) in hESF-GRO medium (Cell Science & Technology Institute) supplemented with the five factors, 0.5 mg/ml fatty acid free bovine ALB (BSA) (Sigma), 10 ng/ml bFGF, and 50 ng/ml Activin A (R&D Systems, Minneapolis, MN) in a humidified atmosphere of 10% CO_2 and 90% air at 37 °C. The medium was refreshed every day.

For induction of hepatoblasts, the human ESC- and iPSC-derived definitive endoderms (day 5) were dissociated with 0.0125% trypsin-0.01325 mmol/l EDTA, and then the trypsin was inactivated with 0.1% soybean trypsin inhibitor (Sigma). The cells were seeded at 1.2×10^5 cells/cm^2 on a laminin-coated 12-well plate with hESF-DIF (Cell Science & Technology Institute) medium supplemented with the five factors, 0.5 mg/ml BSA, 10 ng/ml bFGF, and 50 ng/ml Activin A in a humidified atmosphere of 10% CO_2 and 90% air at 37 °C. The next day, the cells were transduced with 3,000 vector particle/cell of Ad vectors (Ad-HEX and Ad-LacZ) for 1.5 hours in hESF-DIF medium supplemented with the five factors, BSA, 10 ng/ml FGF4 (R&D Systems) and 10 ng/ml BMP4 (R&D Systems).[10] The medium was refreshed every day.

For induction of hepatocytes, human iPSC-derived hepatoblasts in one well (day 9) were passaged onto two wells with 0.0125% trypsin-0.01325 mmol/l EDTA and 0.1% trypsin inhibitor, on type I collagen-coated tissue 12-well plate (15 μg/cm^2) (Nitta Gelatin, Osaka, Japan). The cells were cultured in hepatocyte culture medium supplemented with SingleQuots (Lonza, Walkersville, MD), 10 ng/ml FGF4, 10 ng/ml HGF (R&D Systems), 10 ng/ml Oncostatin M (R&D Systems), and 0.392 ng/ml dexamethasone (Sigma).[11] The medium was refreshed every 2 days.

RNA isolation, RT-PCR, immunostaining, flow cytometry, lacz assay, and assay for cytochrome P4503A4 activity. For details of these procedures, See **Supplementary Materials and Methods**, **Supplementary Tables S1 and S2**.

SUPPLEMENTARY MATERIAL

Figure S1. Characterization of the human ESC (khES1)- and iPSC (Tic)-derived definitive endoderms.

Figure S2. Efficient differentiation of another human iPSC line (Dotcom) into hepatoblasts by overexpression of the *HEX* gene.

Figure S3. Overexpression of *HEX* in the human ESC (khES1)- and iPSC (Tic)-derived definitive endoderms.

© The American Society of Gene & Cell Therapy

Figure S4. Characterization of Ad-HEX-transduced hepatoblasts.
Figure S5. Progression of differentiation of the definitive endoderm to hepatoblasts.
Figure S6. X-gal staining of human iPSC (Tic)-derived definitive endoderms transduced with a conventional or a fiber-modified Ad vector containing the EF-1α promoter.
Figure S7. *HEX* promotes the differentiation into the hepatic lineage, not from undifferentiated iPSCs (Tic), but from iPSC (Tic)-derived definitive endoderm.
Table S1. List of Taqman gene expression assays and primers.
Table S2. List of antibodies used.
Materials and Methods.

ACKNOWLEDGMENTS

We thank Hiroko Matsumura and Midori Hayashida for their excellent technical support. This study was supported by grants from the Ministry of Education, Sports, Science and Technology of Japan (20200076) and by grants from the Ministry of Health, Labor, and Welfare of Japan.

REFERENCES

1. Thomson, JA, Itskovitz-Eldor, J, Shapiro, SS, Waknitz, MA, Swiergiel, JJ, Marshall, VS *et al.* (1998). Embryonic stem cell lines derived from human blastocysts. *Science* **282**: 1145–1147.
2. Takahashi, K, Tanabe, K, Ohnuki, M, Narita, M, Ichisaka, T, Tomoda, K *et al.* (2007). Induction of pluripotent stem cells from adult human fibroblasts by defined factors. *Cell* **131**: 861–872.
3. Makino, H, Toyoda, M, Matsumoto, K, Saito, H, Nishino, K, Fukawatase, Y *et al.* (2009). Mesenchymal to embryonic incomplete transition of human cells by chimeric OCT4/3 (POUSF1) with physiological co-activator EWS. *Exp Cell Res* **315**: 2727–2740.
4. Nagata, TM, Yamaguchi, S, Hirano, K, Makino, H, Nishino, K, Miyagawa, Y *et al.* (2009). Efficient reprogramming of human and mouse primary extra-embryonic cells to pluripotent stem cells. *Genes Cells* **14**: 1395–1404.
5. Lavon, N and Benvenisty, N (2005). Study of hepatocyte differentiation using embryonic stem cells. *J Cell Biochem* **96**: 1193–1202.
6. Khetani, SR and Bhatia, SN (2008). Microscale culture of human liver cells for drug development. *Nat Biotechnol* **26**: 120–126.
7. Baharvand, H, Hashemi, SM and Shahsavani, M (2008). Differentiation of human embryonic stem cells into functional hepatocyte-like cells in a serum-free adherent culture condition. *Differentiation* **76**: 465–477.
8. Hay, DC, Zhao, D, Fletcher, J, Hewitt, ZA, McLean, D, Urruticoechea-Uriguen, A *et al.* (2008). Efficient differentiation of hepatocytes from human embryonic stem cells exhibiting markers recapitulating liver development in vivo. *Stem Cells* **26**: 894–902.
9. Shiraki, N, Umeda, K, Sakashita, N, Takeya, M, Kume, K and Kume, S (2008). Differentiation of mouse and human embryonic stem cells into hepatic lineages. *Genes Cells* **13**: 731–746.
10. Song, Z, Cai, J, Liu, Y, Zhao, D, Yong, J, Duo, S *et al.* (2009). Efficient generation of hepatocyte-like cells from human induced pluripotent stem cells. *Cell Res* **19**: 1233–1242.
11. Agarwal, S, Holton, KL and Lanza, R (2008). Efficient differentiation of functional hepatocytes from human embryonic stem cells. *Stem Cells* **26**: 1117–1127.
12. Si-Tayeb, K, Noto, FK, Nagaoka, M, Li, J, Battle, MA, Duris, C *et al.* (2010). Highly efficient generation of human hepatocyte-like cells from induced pluripotent stem cells. *Hepatology* **51**: 297–305.
13. Duan, Y, Ma, X, Zou, W, Wang, C, Bahbahan, IS, Ahuja, TP *et al.* (2010). Differentiation and characterization of metabolically functioning hepatocytes from human embryonic stem cells. *Stem Cells* **28**: 674–686.
14. Cai, J, Zhao, Y, Liu, Y, Ye, F, Song, Z, Qin, H *et al.* (2007). Directed differentiation of human embryonic stem cells into functional hepatic cells. *Hepatology* **45**: 1229–1239.
15. McLin, VA and Zorn, AM (2006). Molecular control of liver development. *Clin Liver Dis* **10**: 1–25, v.
16. Shiojiri, N (1984). The origin of intrahepatic bile duct cells in the mouse. *J Embryol Exp Morphol* **79**: 25–39.
17. Ingelman-Sundberg, M, Oscarson, M and McLellan, RA (1999). Polymorphic human cytochrome P450 enzymes: an opportunity for individualized drug treatment. *Trends Pharmacol Sci* **20**: 342–349.
18. Hunter, MP, Wilson, CM, Jiang, X, Cong, R, Vasavada, H, Kaestner, KH *et al.* (2007). The homeobox gene Hhex is essential for proper hepatoblast differentiation and bile duct morphogenesis. *Dev Biol* **308**: 355–367.
19. Bogue, CW, Ganea, GR, Sturm, E, Ianucci, R and Jacobs, HC (2000). Hex expression suggests a role in the development and function of organs derived from foregut endoderm. *Dev Dyn* **219**: 84–89.
20. Martinez Barbera, JP, Clements, M, Thomas, P, Rodriguez, T, Meloy, D, Kioussis, D *et al.* (2000). The homeobox gene Hex is required in definitive endodermal tissues for normal forebrain, liver and thyroid formation. *Development* **127**: 2433–2445.
21. Keng, VW, Yagi, H, Ikawa, M, Nagano, T, Myint, Z, Yamada, K *et al.* (2000). Homeobox gene Hex is essential for onset of mouse embryonic liver development and differentiation of the monocyte lineage. *Biochem Biophys Res Commun* **276**: 1155–1161.
22. Bort, R, Signore, M, Tremblay, K, Martinez Barbera, JP and Zaret, KS (2006). Hex homeobox gene controls the transition of the endoderm to a pseudostratified, cell emergent epithelium for liver bud development. *Dev Biol* **290**: 44–56.
23. Xu, ZL, Mizuguchi, H, Sakurai, F, Koizumi, N, Hosono, T, Kawabata, K *et al.* (2005). Approaches to improving the kinetics of adenovirus-delivered genes and gene products. *Adv Drug Deliv Rev* **57**: 781–802.
24. Tashiro, K, Inamura, M, Kawabata, K, Sakurai, F, Yamanishi, K, Hayakawa, T *et al.* (2009). Efficient adipocyte and osteoblast differentiation from mouse induced pluripotent stem cells by adenoviral transduction. *Stem Cells* **27**: 1802–1811.
25. Tashiro, K, Kawabata, K, Sakurai, H, Kurachi, S, Sakurai, F, Yamanishi, K *et al.* (2008). Efficient adenovirus vector-mediated PPAR gene transfer into mouse embryoid bodies promotes adipocyte differentiation. *J Gene Med* **10**: 498–507.
26. Kubo, A, Chen, V, Kennedy, M, Zahradka, E, Daley, GQ and Keller, G (2005). The homeobox gene HEX regulates proliferation and differentiation of hemangioblasts and endothelial cells during ES cell differentiation. *Blood* **105**: 4590–4597.
27. Kovesdi, I, Brough, DE, Bruder, JT and Wickham, TJ (1997). Adenoviral vectors for gene transfer. *Curr Opin Biotechnol* **8**: 583–589.
28. Kawabata, K, Sakurai, F, Yamaguchi, T, Hayakawa, T and Mizuguchi, H (2005). Efficient gene transfer into mouse embryonic stem cells with adenovirus vectors. *Mol Ther* **12**: 547–554.
29. Koizumi, N, Mizuguchi, H, Utoguchi, N, Watanabe, Y and Hayakawa, T (2003). Generation of fiber-modified adenovirus vectors containing heterologous peptides in both the HI loop and C terminus of the fiber knob. *J Gene Med* **5**: 267–276.
30. Asahina, K, Fujimori, H, Shimizu-Saito, K, Kumashiro, Y, Okamura, K, Tanaka, Y *et al.* (2004). Expression of the liver-specific gene Cyp7a1 reveals hepatic differentiation in embryoid bodies derived from mouse embryonic stem cells. *Genes Cells* **9**: 1297–1308.
31. Moll, R, Franke, WW, Schiller, DL, Geiger, B and Krepler, R (1982). The catalog of human cytokeratins: patterns of expression in normal epithelia, tumors and cultured cells. *Cell* **31**: 11–24.
32. D'Amour, KA, Agulnick, AD, Eliazer, S, Kelly, OG, Kroon, E and Baetge, EE (2005). Efficient differentiation of human embryonic stem cells to definitive endoderm. *Nat Biotechnol* **23**: 1534–1541.
33. Touboul, T, Hannan, NR, Corbineau, S, Martinez, A, Martinet, C, Branchereau, S *et al.* (2010). Generation of functional hepatocytes from human embryonic stem cells under chemically defined conditions that recapitulate liver development. *Hepatology* **51**: 1754–1765.
34. Vallier, L, Touboul, T, Brown, S, Cho, C, Bilican, B, Alexander, M *et al.* (2009). Signaling pathways controlling pluripotency and early cell fate decisions of human induced pluripotent stem cells. *Stem Cells* **27**: 2655–2666.
35. Shiraki, N, Yoshida, T, Araki, K, Umezawa, A, Higuchi, Y, Goto, H *et al.* (2008). Guided differentiation of embryonic stem cells into Pdx1-expressing regional-specific definitive endoderm. *Stem Cells* **26**: 874–885.
36. Morrison, GM, Oikonomopoulou, I, Migueles, RP, Soneji, S, Livigni, A, Enver, T *et al.* (2008). Anterior definitive endoderm from ESCs reveals a role for FGF signaling. *Cell Stem Cell* **3**: 402–415.
37. Sumi, T, Tsuneyoshi, N, Nakatsuji, N and Suemori, H (2008). Defining early lineage specification of human embryonic stem cells by the orchestrated balance of canonical Wnt/beta-catenin, Activin/Nodal and BMP signaling. *Development* **135**: 2969–2979.
38. Xu, RH, Peck, RM, Li, DS, Feng, X, Ludwig, T and Thomson, JA (2005). Basic FGF and suppression of BMP signaling sustain undifferentiated proliferation of human ES cells. *Nat Methods* **2**: 185–190.
39. Keller, G (2005). Embryonic stem cell differentiation: emergence of a new era in biology and medicine. *Genes Dev* **19**: 1129–1155.
40. Selden, C, Sharif, A, McCloskey, P, Ryder, T, Roberts, E and Hodgson, H (1999). Three-dimensional *in vitro* cell culture leads to a marked upregulation of cell function in human hepatocyte cell lines–an important tool for the development of a bioartificial liver machine. *Ann N Y Acad Sci* **875**: 353–363.
41. Soto-Gutiérrez, A, Navarro-Alvarez, N, Zhao, D, Rivas-Carrillo, JD, Lebkowski, J, Tanaka, N *et al.* (2007). Differentiation of mouse embryonic stem cells to hepatocyte-like cells by co-culture with human liver nonparenchymal cell lines. *Nat Protoc* **2**: 347–356.
42. Kubo, A, Kim, YH, Irion, S, Kasuda, S, Takeuchi, M, Ohashi, K *et al.* (2010). The homeobox gene Hex regulates hepatocyte differentiation from embryonic stem cell-derived endoderm. *Hepatology* **51**: 633–641.
43. Hacein-Bey-Abina, S, Von Kalle, C, Schmidt, M, McCormack, MP, Wulffraat, N, Leboulch, P *et al.* (2003). LMO2-associated clonal T cell proliferation in two patients after gene therapy for SCID-X1. *Science* **302**: 415–419.
44. Sakamoto, N, Tsuji, K, Muul, LM, Lawler, AM, Petricoin, EF, Candotti, F *et al.* (2007). Bovine apolipoprotein B-100 is a dominant immunogen in therapeutic cell populations cultured in fetal calf serum in mice and humans. *Blood* **110**: 501–508.
46. Furue, MK, Na, J, Jackson, JP, Okamoto, T, Jones, M, Baker, D *et al.* (2008). Heparin promotes the growth of human embryonic stem cells in a defined serum-free medium. *Proc Natl Acad Sci USA* **105**: 13409–13414.
47. Mizuguchi, H and Kay, MA (1998). Efficient construction of a recombinant adenovirus vector by an improved *in vitro* ligation method. *Hum Gene Ther* **9**: 2577–2583.
48. Mizuguchi, H and Kay, MA (1999). A simple method for constructing E1- and E1/E4-deleted recombinant adenoviral vectors. *Hum Gene Ther* **10**: 2013–2017.
49. Maizel, JV Jr, White, DO and Scharff, MD (1968). The polypeptides of adenovirus. I. Evidence for multiple protein components in the virion and a comparison of types 2, 7A, and 12. *Virology* **36**: 115–125.
50. Suemori, H, Yasuchika, K, Hasegawa, K, Fujioka, T, Tsuneyoshi, N and Nakatsuji, N (2006). Efficient establishment of human embryonic stem cell lines and long-term maintenance with stable karyotype by enzymatic bulk passage. *Biochem Biophys Res Commun* **345**: 926–932.

This work is licensed under the Creative Commons Attribution-NonCommercial-Share Alike 3.0 Unported License. To view a copy of this license, visit http://creativecommons.org/licenses/by-nc-sa/3.0/

TISSUE ENGINEERING: Part C
Volume 16, Number 4, 2010
© Mary Ann Liebert, Inc.
DOI: 10.1089/ten.tec.2009.0459

Development of a New Assay System for Evaluating the Permeability of Various Substances Through Three-Dimensional Tissue

Yuji Haraguchi, Ph.D.,[1,*] Waki Sekine, M.Sc.,[1,*] Tatsuya Shimizu, M.D., Ph.D.,[1,*] Masayuki Yamato, Ph.D.,[1] Shunichiro Miyoshi, M.D., Ph.D.,[2] Akihiro Umezawa, M.D., Ph.D.,[3] and Teruo Okano, Ph.D.[1]

A novel assay system with cell-dense three-dimensional (3D) tissue was developed for measuring the permeability of substances. In this paper, the permeabilities of various molecules containing nutrients, a cytokine, and a chemokine were examined and analyzed. A single-layered cell sheet was approximately 20 μm thick, and as the number of layers of these cell sheets increased, so did the total thickness of the tissue. The diffusion rates of glucose and pyruvic acid were reduced to approximately 30–40% by a single-layered cell sheet compared with the control without the cell sheet, and the diffusion of both substances were completely inhibited by a quadruple-layered cell sheet. The diffusion rate of creatinin was reduced to approximately 50% and 15–20% by a single-layered and by a quintuplet-layered cell sheet, respectively. On the other hand, the diffusion rate of stromal cell–derived factor 1α, vascular endothelial growth factor, β2-microglobulin, and transferrin was reduced to approximately 10%, 5%, 20%, and 10%, by only a single-layered cell sheet, respectively. The diffusion of these substances were completely inhibited by a double-layered cell sheet. These results show that the permeability of substances through 3D tissue significantly decreased with the increase of the molecular weight. Therefore, the system could give a simulated living-tissue condition for measuring the permeability of substances. To our knowledge, this is the first report about measuring the permeability of substances through cell-dense 3D tissues without scaffolds. The assay system is believed to contribute to the progress of physiology, metabology, biochemistry, and pharmacokinetics. Further, the system may give some hints for developing a new dialysis membrane technology for an artificial kidney.

Introduction

THERE ARE MANY REPORTS that described the adverse effects, the permeability, and the uptakes of various substances, including nutrients and drugs, by *in vitro* cell assay systems, which were designed and used model systems for the heart tissue, the small intestinal mucosa, the oral mucosa, the blood–brain barrier, the blood–retinal barrier, and so on.[1–6] These assay systems are essential in the field of pharmacokinetics as well as in the understanding of biochemistry, physiology, and metabology of tissues and organs. An adequate assay system has a clear advantage as *in vitro* models that could require no animal experiments. To date, experiments in these fields have relied on assays using two-dimensional (2D) single-layered cell cultures. Two-dimensional culture system is too simple in comparison with actual living tissues or organs. Cells of 2D culture system are significantly different from that of three-dimensional (3D) culture system in terms of their morphology, cell-to-cell interactions, surrounding extracellular matrix, proliferation rates, and differentiation.[7–9] These differences may affect their gene expression and other biological activities. It is believed that 3D culture system can simulate *in vivo* situations.[7,10,11] An *in vitro* assay system using 3D tissues would, therefore, be clearly desirable in the fields described above.

Three-dimensional tissues can be re-constructed *in vitro* using tissue engineering techniques.[12] Conventional tissue engineering has employed 3D scaffolds (e.g., polyglycolic acid, collagen gel, and gelatin) that are useful as alternatives for extracellular matrix, and cells are seeded into the scaffolds. However, 3D tissues fabricated by using the scaffolds are extremely cell-sparse tissues because of insufficient cell migration into the scaffolds.[13,14] In an attempt to improve this situation, our laboratory has created and utilized an original

[1]Institute of Advanced Biomedical Engineering and Science, TWIns, Tokyo Women's Medical University, Tokyo, Japan.
[2]Department of Cardiology, Keio University School of Medicine, Tokyo, Japan.
[3]Department of Reproductive Biology and Pathology, National Research Institute for Child Health and Development, Tokyo, Japan.
*These three authors contributed equally to this study.

technology called cell sheet engineering,[15] which can prepare 3D tissues without the scaffolds by layering cell sheets harvested from temperature-responsive culture dishes.[16–19] This method allows cell harvest to require no proteolytic treatments and to preserve cell-to-cell connections completely.[20,21] The technique also can control the thickness of re-constructed 3D tissues by manipulating the number of cell layers. Therefore, 3D tissues fabricated by the cell sheet engineering are suitable as an *in vitro* cell-dense 3D tissue model.

In this study, we develop a new assay system that uses cell-dense 3D tissues made by the cell sheet engineering in conjunction with a modified cell culture insert, and measured the permeability of various substances, including nutrients, a cytokine, and a chemokine, through the cell-dense 3D tissues for verifying the usefulness of the system.

Materials and Methods

Culture of C2C12 mouse skeletal myoblast cell lines and human endometrial gland–derived mesenchymal cells

C2C12 mouse skeletal myoblast cell lines were purchased from Dainippon Sumitomo Pharma (Osaka, Japan). C2C12 cells and human endometrial gland–derived mesenchymal cells (EMCs)[22] were cultured in Dulbecco's modified Eagle's medium (DMEM; Sigma-Aldrich Japan, Tokyo) supplemented with 10% fetal bovine serum (Japan Bio Serum, Nagoya, Japan) and 1% penicillin and streptomycin (Invitrogen, Carlsbad, CA). These cells were cultured at 37°C in a humidified atmosphere with 5% CO_2.

A device for permeability experiments

A device was developed by modifying a cell culture insert (the membrane pore size: 3 μm; Becton, Dickinson and Company, Franklin Lakes, NJ) as shown in Fig. 1. Briefly, a round polyethylene terephthalate film (diameter: 30 mm) having a hole in its center (diameter: 5 mm) was glued to the outside-bottom of the membrane of the cell culture insert with cyanoacrylate adhesive (Toagosei, Tokyo, Japan) (Fig. 1). A single cell sheet or a several layered cell sheet was then placed on the bottom of the device, covering the permeance hole, as described in detail below (Fig. 2A–E). Thus, substances in the upper medium could diffuse only through the cell sheets and the permeance hole.

Preparation of cell sheets and the manipulation of the cell sheets into layered constructs

Cell suspensions were plated onto a 35 mm temperature-responsive culture dish (Upcell; CellSeed, Tokyo, Japan) at 6×10^5 cells/dish (for C2C12 cells) or 1×10^6 cells/dish (for EMCs). After 3 days (C2C12 cells) or 4 days (EMCs), the culture dishes were placed in a separate CO_2 incubator set at 20°C. Each cell sheet with its medium was gently aspirated into a tip of a pipette and put on the bottom membrane of the device one at a time. An additional medium was then poured into the upper part of the device, having the cell sheet for spreading out any folded portions. Once the cell sheet was spread out, the medium was aspirated away, and the device was incubated for 60 min at 37°C to allow the cell sheet to fully adhere to the bottom membrane of the device. Cell sheets were layered by repeating the following procedure: detaching another cell sheet from a temperature-responsive culture dish and stacking it onto the first cell sheet. In this manner, triple-, quadruple-, and quintuple-layered constructs were created. After 60 min incubation, a fresh medium was added to the device's upper and lower parts, and the device was incubated at 37°C for 24 h. Upon the end of the incubation, the culture media of the upper and lower parts were separately collected and were used for chemical and protein analyses, and enzyme-linked immunosorbent assay (ELISA). The volumes of the upper and lower media were also measured.

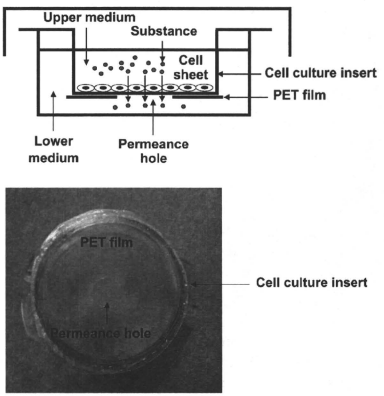

FIG. 1. A device to measure the permeability of substances. A schematic illustration of the device as viewed from the side is shown in (**A**). (**B**) is a photograph as viewed from the bottom.

Histological analysis

Cell sheets on the device were fixed with 4% paraformaldehyde. Specimens were embedded in paraffin, sectioned, and stained with hematoxylin and eosin. Prepared specimens were examined by a microscope (Elipse TE2000-U; Nikon, Tokyo, Japan).

Medium, chemical, and proteins

Glucose/pyruvic acid–deficient DMEM was purchased from Invitrogen; creatinin, human β2-microglobulin, and human transferrin were from Wako Pure Chemicals (Tokyo, Japan); human vascular endothelial growth factor (VEGF) and human stromal–derived factor 1α (SDF-1α) were from Funakoshi (Tokyo, Japan).

Chemical and protein analyses, and ELISA

Concentrations of glucose, pyruvic acid, and creatinin were measured by the hexokinase UV method,[23] the pyruvate oxidase method,[24] and an enzymatic method by SRL (Tokyo, Japan), respectively. Concentrations of β2-microglobulin and transferrin were measured by a latex agglutination test (SRL).

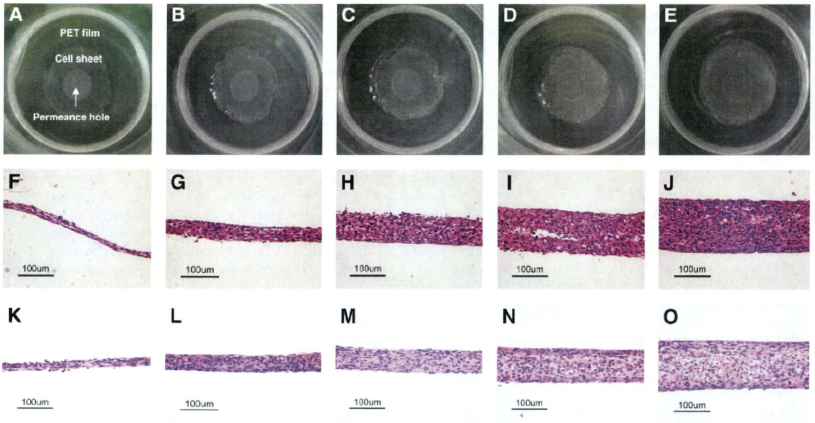

FIG. 2. Morphological and histological observation of single cell sheets and of cell sheets with several layers. The photograph (**A**) shows a monolayer EMC sheet on a new device; (**B**), a double-layered EMC sheet; (**C**), a triple-layered EMC sheet; (**D**), a quadruple-layered EMC sheet; and (**E**), a quintuplet-layered EMC sheet. Cross-sectional observation of layered C2C12 cell sheets (**F–J**) and EMC sheets (**K–O**). Photographs (**F**) and (**K**) show single-layered cell sheets; (**G**) and (**L**), double-layered cell sheets; (**H**) and (**M**), triple-layered cell sheets; (**I**) and (**N**), quartet-layered cell sheets; (**J**) and (**O**), quintet-layered cell sheets. Scale bars indicate 100 μm.

Amounts of human VEGF and SDF-1α were quantitated by a commercially available ELISA kit (Funakoshi).

Relative permeability and relative residual amount of each substance

Permeability of each substance was calculated by the following equation:

$$\text{Permeability} = \frac{\text{The concentration of a substance in the lower medium}}{\text{The volume of the lower medium}} \times 100$$

For comparison, the permeability of a substance without a cell sheet was assumed to be 100% (the control permeability), and its relative permeability through a cell sheet was calculated by the following equation:

$$\text{Relative permeability} = \frac{\text{The permeability of a substance through a cell sheet}}{\text{The control permeability}} \times 100$$

The residual amount of a substance was calculated by the following equation:

Residual amount = [the amount of a substance remaining in the upper medium after incubation for 24 h] + [the amount of a substance in the lower medium after incubation for 24 h].

The residual amount without the cell sheet was estimated at 100% (the control residual amount). Relative residual amounts were then calculated for substances by the following equation:

$$\text{Relative residual amount} = \frac{\text{The residual amount of a substance for 24 h with cell sheet}}{\text{The control residual amount}} \times 100$$

Data are expressed as mean ± SD.

Results

Morphologic analysis of cell sheets

The cross sections of single-layered and multi-layered cell sheets were observed. When the culture temperature was decreased from 37°C to 20°C, C2C12 cells or EMCs on a temperature-responsive culture dish were detached as a contiguous cell sheet. Those cell sheets shrunk horizontally due to the cytoskeletal tensile reorganization. As a result, those cell sheets consisted of two or three cell layers, and the thickness of the cell sheets became approximately 20 μm (Fig. 2F, K). The addition of a layered cell sheet to a tissue increased the total tissue's thickness by the thickness of the added cell sheet (Fig. 2F–J, the C2C12 cell sheet; Fig. 2K–O, the EMC sheet). These results show that cell sheet engineering can control the thickness of 3D tissues.

Permeability of the substances through layered cell sheets

Because nutrients (pyruvic acid and glucose) are vital for living tissues, the permeability through the 3D tissue is a basic factor for tissue engineering. Therefore, our first experiments assessed the permeability of the nutrients through

C2C12 cell sheets by adding DMEM into the upper section of the device and glucose/pyruvic acid–deficient DMEM into the lower part. The permeabilities of pyruvic acid and glucose were inhibited by approximately 60% (in other words, it was reduced to approximately 40%) by a single-layered C2C12 cell sheet (Fig. 3A, B). As the number of layered cell sheets increased, the permeabilities of pyruvic acid and glucose decreased. Almost complete inhibition of the permeability was observed upon the use of a quadruple-layered or a quintuple-layered cell sheet (Fig. 3A, B). Similar results were also observed using EMC sheets (Fig. 3D, E).

In the next set of experiments, the permeabilities of creatinin, β2-microgloblin, and transferrin were examined, because these are important substances for measuring the kidney glomerulus function.[25,26] DMEM containing creatinin, β2-microglobulin, or transferrin was added to the upper part of the device, while DMEM without these substances was added to the lower part. The permeability of creatinin was inhibited by approximately 50% by a single-layered C2C12 cell sheet (Fig. 3C). Again, as the number of layered cell sheets increased, the sheets' collective inhibitory effects increased. The permeability of creatinin was inhibited by approximately 85% by a quintuple-layered cell sheet (Fig. 3C). On the other hand, the permeabilities of β2-microglobulin and transferrin were inhibited by approximately 80% and 90% by only a single-layered C2C12 cell sheet, respectively, and both were almost completely inhibited by a double-layered cell sheet (Fig. 4A, B). Similar results were also observed using EMC sheets (Figs. 3F and 4D, E).

In the third set of experiments, the permeabilities of VEGF and SDF-1α were examined, because these substances are important in the regeneration of tissues.[27,28] DMEM containing either SDF-1α or VEGF was added to the upper part of the device, while DMEM was added to the lower part. C2C12 cells secreted SDF-1α, and EMCs secreted VEGF, but not SDF-1α (data not shown). A human-specific VEGF ELISA kit, which is unable to cross react with mouse VEGF, was used to detect VEGF. Therefore, only C2C12 cell sheets were used for determining the permeability of VEGF, and only EMC sheets were used for determining the permeability of SDF-1α. The permeability of VEGF was inhibited by approximately 95% (in other words, it was reduced to 5%) by a single-layered C2C12 cell sheet and was almost completely inhibited by a double-layered cell sheet (Fig. 4C). Likewise, the permeability of SDF-1α was inhibited by approximately 90% by a single-layered EMC sheet and was almost completely inhibited by a double-layered cell sheet (Fig. 4F).

The rate of consumption of glucose and pyruvic acid increased as the number of cell sheets increased. Once tissues had more than triple-layered cell sheets, the increase of the rate slowed (Fig. 5A, B). Similar tendency was also observed in the experiments using EMC sheets (Fig. 5C, D). In contrast, the amount of creatinin, SDF-1α, VEGF, β2-microglobulin, and transferrin was hardly changed during incubation with layered cell sheets (data not shown).

Discussion

Many reports have already been published regarding the permeability and uptake of various substances through a single-layered of cells.[1–5] The present study is unique and original because our new assay system can measure the permeability of substances through cell-dense 3D tissues rather than a single-layered of cells. The cell-dense 3D tissue was prepared by cell sheet engineering, and the device was made by our laboratory.

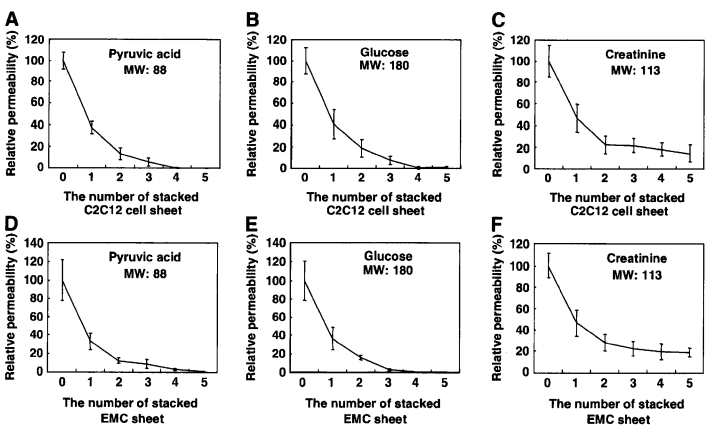

FIG. 3. Permeability of low-molecular-weight substances. The graph (A) shows pyruvic acid experiment through C2C12 cell sheets; (B), glucose; and (C), creatinin. The graph (D) shows pyruvic acid experiment through EMC sheets; (E), glucose; and (F), creatinin. The data are expressed as mean ± SD ($n = 4$).

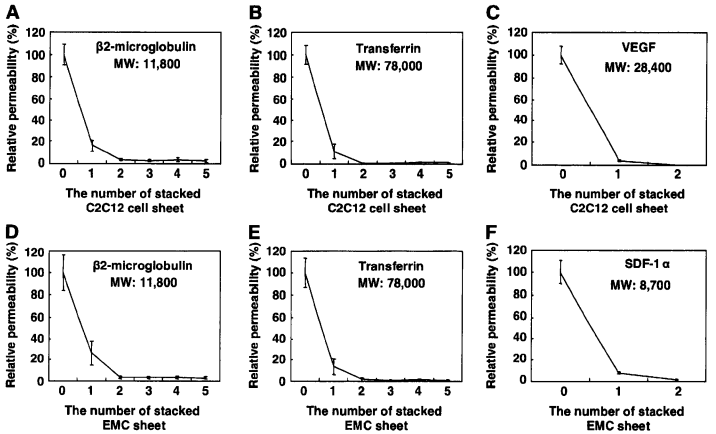

FIG. 4. Permeability of high-molecular-weight substances. The graph (A) shows β2-microglobulin experiment through C2C12 cell sheets; (B), transferrin; and (C), VEGF. The graph (D) shows β2-microglobulin experiment through EMC sheets; (E), transferrin; and (F), SDF-1α. The data are expressed as mean ± SD ($n = 4$).

First, we used our assay system to examine the permeability of nutrients across 3D tissues (Fig. 3). The results suggested that the cells that were separated from their nutrient source by more than triple-layered cell sheets were severely starved of nutrients. Both *in vivo* and *in vitro*, cell death was found to be common in engineered tissues of more than triple-layered cell sheets, though the same kinds of cells usually survive without necrosis in tissues consisting of a single-, a double-, or a triple-layered cell sheet[29] (Sekine, W., Haraguchi, Y., Shimizu, T., Umezawa, A., and Okano, T.,

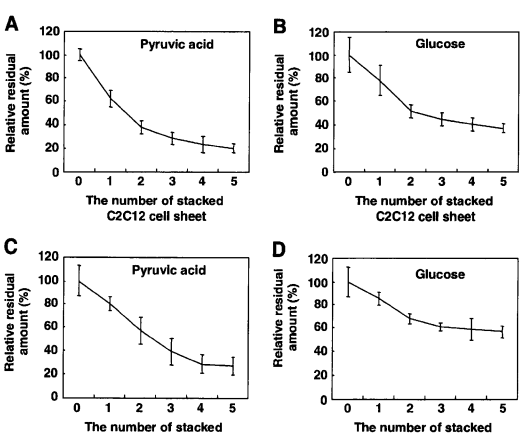

FIG. 5. Consumption of nutrients during incubation with layered cell sheets. The graph (A) shows relative residual amount of pyruvic acid after incubation with C2C12 cell sheets, and (B) shows that of glucose. The graph (C) shows relative residual amount of pyruvic acid after incubation with EMC sheets, and (D) shows that of glucose. The amounts of substances taken after 24 h without the cell sheet were assumed to be 100%. The data are expressed as mean ± SD ($n = 4$).

unpublished observation). Our results suggested that insufficient diffusion of nutrients induces a rapid cell death in the thick tissues. Other reports, in contrast, have claimed that glucose could penetrate into 3D tissues via a scaffold containing skeletal muscle myoblasts.[30] The report showed that glucose concentrations only decreased from 4.28 mmol/L at the edge of the tissue to 3.18 mmol/L at the depth of 2 mm.[30] This result is profoundly different from ours; the inconsistency is probably due to different cell densities of 3D tissues of the two studies. In this study, 3D tissues, which were fabricated by cell sheet engineering, were constructed without 3D scaffolds described above and were, therefore, very cell dense. In contrast, in the reported study, 3D tissues fabricated using scaffolds were very cell sparse due to insufficient cell migration into the scaffolds. Nevertheless, both our study and that of Davis *et al.*[30] present important data that are relevant to the field of tissue metabology.

In another set of experiments, the permeability of high-molecular-weight substrates (SDF-1α, VEGF, β2-microglobulin, and transferrin) was completely inhibited by a double-layered cell sheet. These results show that cells in tissues that are only one or two layers thick can be deficient in growth factors or cytokines. We propose that the formation of functional microvessels is necessary to supply these large molecules into the interiors of 3D tissues. On the other hand, VEGF and SDF-1α have received a great deal of attention from the field of regenerative medicine.[27,28] The former is intimately involved in angiogenesis, and the latter with stem cell homing. In fact, VEGF has even been used in clinical therapy, and in animal experiment; SDF-1α could improve myocardial function after infarction.[26,28] It is thought that the effectiveness of these factors depends on the efficiency of diffusion into the treated area. In the present study, we showed that these factors were unable to diffuse efficiently into the cell-dense tissues. Thus, the successful implementation of cytokine therapy will require a development of techniques that can help these factors diffuse efficiently. Our assay system using cell-dense 3D tissues may be useful for the development of efficient cytokine therapy.

In this article, the permeability of substances through cell-dense 3D tissue was shown to be significantly reduced depending on the molecular weight (Figs. 3 and 4). This observation agrees with a report that the permeability of mannitol (molecular weight: 182) through a single-layered of brain capillary endothelial cell lines on a cell culture insert was approximately twice as great as that of inulin (molecular weight: 5,000).[2] These results showed that the permeability of substances through 2D cell culture and 3D tissues was significantly reduced with the increase of molecular weight, and that our assay system is feasible as an assay system to measure the permeability of substances through 3D tissues.

Drug development requires the development of *in vitro* assay systems that simulate actual living tissues and organs. In addition, an adequate assay system has a clear advantage as an *in vitro* model that require no animal experiments. The researcher should try as much as possible to replace the animal model with an alternative nonanimal model.[31] It is generally thought that 3D culture systems resemble *in vivo* situations much more closely than 2D culture systems.[7,10,11] Cell sheet engineering gives the fabrication of cell-dense 3D tissues without biodegradable scaffolds. Therefore, for example, layered cardiomyocyte sheets interact directly with each other and can couple electrically, resulting in synchronously beating 3D myocardial tissues *in vitro*.[32,33] *In vivo* subcutaneous transplantation of layer cardiomyocyte sheets also demonstrated that these synchronously beating heart-like tissues survive for over 1 year.[33] Our *in vitro* 3D assay system using cell sheet engineering is thought to be proper for *in vivo* situation. Therefore, our assay system has potential to reduce animal experiment. In addition, the cell sheet engineering also enables the fabrication of complicated heterogeneous tissues. In fact, our laboratory previously reported about heterogeneous 3D coculture comprising hepatocytes and endothelial cells using the technique.[34] The hepatocytes of the 3D culture system showed a differentiated cell shape and the extensive albumin expression of hepatocytes, which were never seen in hepatocyte monoculture.[34] Combination of our assay system and heterogeneous layering cell sheets can allow us to analyze pharmacologically and pharmacokinetically complicated 3D tissues such as the blood–brain barrier, the small intestinal mucosa, and the kidney glomerulus. For example, the blood–brain barrier model can be fabricated by a combination of an endothelial cell sheet, a pericyte sheet, and an astrocyte sheet.

Several novel therapies containing a hybrid bioartificial kidney for the treatment of kidney failure are tried clinically.[35] The hybrid bioartificial kidney is combined with dialysis membrane and cells. In this study a device by modifying a cell culture insert was used. By the replacement of the device dialysis membrane and cell sheet, a new hybrid-type artificial kidney model device can also be fabricated easily. Therefore, our assay system may be applied in the field of dialysis membrane technology.

Conclusions

We have developed a new model system that measures the permeability of substances through cell-dense 3D tissues using cell sheet engineering and a modified cell culture insert, and analyzed in detail the permeability of various molecules. It has been shown that our assay system is feasible as an assay system to measure the permeability of substances through 3D tissues using substances that have various molecular weights. This is the first report about measuring the permeability of substances through cell-dense 3D tissues without scaffolds. The thickness of the tissues can be also controlled easily as shown in Figure 2. Our assay system represents a significant advancement and offers much exciting potential in the fields of biochemistry, physiology, metabology of tissues, cytokine therapy, drug development, and dialysis membrane technology.

Acknowledgments

We appreciate the useful comments and technical criticism of Drs. Norio Ueno and Noriaki Matsuda (Institute of Advanced Biomedical Engineering and Science, Tokyo Women's Medical University). This work was supported by grants from the 21COE program and the High-Tech Research Center Program from the Ministry of Education, Culture, Sports, Science, and Technology; grants from the Japan Society for the Promotion of Science; Research Grants for Cardiovascular Disease and Regenerative Medicine from the

Ministry of Health, Labour, and Welfare; and the Open Research Grant from the Japanese Research Promotion Society for Cardiovascular Diseases.

Disclosure Statement

No competing financial interests exist.

References

1. Hilgers, A.R., Conradi, R.A., and Burton, P.S. Caco-2 cell monolayers as a model for drug transport across the intestinal mucosa. Pharm Res **7,** 902, 1990.
2. Hosoya, K., Tetsuka, K., Nagase, K., Tomi, M., Saeki, S., Ohtsuki, S., Takanaga, H., Yanai, N., Obinata, M., Kikuchi, A., Okano, T., and Terasaki, T. Conditionally immortalized brain capillary endothelial cell lines established from a transgenic mouse harboring temperature-sensitive simian virus 40 large T-antigen gene. AAPS Pharm Sci **2,** E27, 2000.
3. Kimura, T., Yamano, H., Tanaka, A., Matsumura, T., Ueda, M., Ogawara, K., and Higaki, K. Transport of D-glucose across cultured stratified cell layer of human oral mucosal cells. J Pharm Pharmacol **54,** 213, 2002.
4. Roux, F., and Couraud, P.O. Rat brain endothelial cell lines for the study of blood-brain barrier permeability and transport functions. Cell Mol Neurobiol **25,** 41, 2005.
5. Tomi, M., Terayama, T., Isobe, T., Egami, F., Morito, A., Kurachi, M., Ohtsuki, S., Kang, Y.S., Terasaki, T., and Hosoya, K. Function and regulation of taurine transport at the inner blood-retinal barrier. Microvasc Res **73,** 100, 2007.
6. Mukhopadhyay, P., Rajesh, M., Bátkai, S., Kashiwaya, Y., Haskó, G., Liaudet, L., Szabó, C., and Pacher, P. Role of superoxide, nitric oxide, and peroxynitrite in doxorubicin-induced cell death *in vivo* and *in vitro*. Am J Physiol Heart Circ Physiol **296,** 1466, 2009.
7. Abbott, A. Biology's new dimension. Nature **424,** 870, 2003.
8. Brännvall, K., Bergman, K., Wallenquist, U., Svahn, S., Bowden, T., Hilborn, J., and Forsberg-Nilsson, K. Enhanced neuronal differentiation in a three-dimensional collagen-hyaluronan matrix. J Neurosci Res **85,** 2138, 2007.
9. Liu, H., Collins, S.F., and Suggs, L.J. Three-dimensional culture for expansion and differentiation of mouse embryonic stem cells. Biomaterials **27,** 6004, 2006.
10. Editorial. Goodbye, flat biology? Nature **424,** 861, 2003.
11. Smalley, K.S., Lioni, M., and Herlyn, M. Life isn't flat: taking cancer biology to the next dimension. In Vitro Cell Dev Biol Anim **42,** 242, 2006.
12. Langer, R., and Vacanti, J.P. Tissue engineering. Science **260,** 920, 1993.
13. Leor, J., Aboulafia-Etzion, S., Dar, A., Shapiro, L., Barbash, I.M., Battler, A., Granot, Y., and Cohen, S. Bioengineered cardiac grafts: a new approach to repair the infracted myocardium? Circulation **100(suppl II),** II63, 1999.
14. Sakai, T., Li, R.K., Weisel, R.D., Mickle, D.A., Kim, E.T., Jia, Z.Q., and Yau, T.M. The fate of a tissue-engineered cardiac graft in the right ventricular outflow tract of the rat. J Thorac Cardiovasc Surg **121,** 932, 2001.
15. Yamato, M., and Okano, T. Cell sheet engineering. Materials Today **7, 42,** 2004.
16. Yamada, N., Okano, T., Sakai, H., Karikusa, F., Sawasaki, Y., and Sakurai, Y. Thermo-responsive polymeric surface: control of attachment and detachment of cultured cells. Makromol Chem Rapid Commun **11,** 571, 1990.
17. Okano, T., Yamada, N., Sakai, H., and Sakurai, Y. A novel recovery system for cultured cells using plasma-treated polystyrene dishes grafted with poly (N-isopropylacrylamide). J Biomed Mater Res **27,** 1243, 1993.
18. Yang, J., Yamato, M., Shimizu, T., Sekine, H., Ohashi, K., Kanzaki, M., Ohki, T., Nishida, K., and Okano, T. Reconstruction of functional tissues with cell sheet engineering. Biomaterials **28,** 5033, 2007.
19. Matsuda, N., Shimizu, T., Yamato, M., and Okano, T. Tissue engineering based on cell sheet technology. Adv Mater **19,** 3089, 2007.
20. Yamato, M., Utsumi, M., Kushida, A., Konno, C., Kikuchi, A., and Okano, T. Thermo-responsive culture dishes allow the intact harvest of multilayered keratinocyte sheets without dispase by reducing temperature. Tissue Eng **7,** 473, 2001.
21. Nishida, K., Yamato, M., Hayashida, Y., Watanabe, K., Maeda, N., Watanabe, H., Yamamoto, K., Nagai, S., Kikuchi, A., Tano, Y., and Okano, T. Functional bioengineered corneal epithelial sheet grafts from corneal stem cells expanded *ex vivo* on a temperature-responsive cell culture surface. Transplantation **77,** 379, 2004.
22. Hida, N., Nishiyama, N., Miyoshi, S., Kira, S., Segawa, K., Uyama, T., Mori, T., Miyado, K., Ikegami, Y., Cui, C., Kiyono, T., Kyo, S., Shimizu, T., Okano, T., Sakamoto, M., Ogawa, S., and Umezawa, A. Novel cardiac precursor-like cells from human menstrual blood-derived mesenchymal cells. Stem Cells **26,** 1695, 2008.
23. Koch, C.D. Determination of glucose with glucoseoxidase-UV, using hexokinase as the reference method. J Clin Chem Clin Biochem **14,** 373, 1976.
24. Valero, E., and García-Carmona, F. Optimizing enzymatic cycling assays: spectrophotometric determination of low levels of pyruvate and L-lactate. Anal Biochem **239,** 47, 1996.
25. Boron, W.F., and Boulpaep, E.L. Medical Physiology. Philadelphia, PA: Elsevier Science, 2003.
26. Branten, A.J., Swinkels, D.W., Klasen, I.S., and Wetzels, J.F. Serum ferritin levels are increased in patients with glomerular diseases and proteinuria. Nephrol Dial Transplant **19,** 2754, 2004.
27. Tang, J., Wang, J., Song, H., Huang, Y., Yang, J., Kong, X., Guo, L., Zheng, F., and Zhang, L. Adenovirus-mediated stromal cell-derived factor-1 alpha gene transfer improves cardiac structure and function after experimental myocardial infarction through angiogenic and antifibrotic actions. Mol Biol Rep (in press).
28. Gaffney, M.M., Hynes, S.O., Barry, F., and O'Brien, T. Cardiovascular gene therapy: current status and therapeutic potential. Br J Pharmacol **152,** 175, 2007.
29. Shimizu, T., Sekine, H., Yang, J., Isoi, Y., Yamato, M., Kikuchi, A., Kobayashi, E., and Okano, T. Polysurgery of cell sheet grafts overcomes diffusion limits to produce thick, vascularized myocardial tissues. FASEB J **20,** 708, 2006.
30. Davis, B.H., Schroeder, T., Yarmolenko, P.S., Guilak, F., Dewhirst, M.W., and Taylor, D.A. An *in vitro* system to evaluate the effects of ischemia on survival of cells used for cell therapy. Ann Biomed Eng **35,** 1414, 2007.
31. Vitale, A., Manciocco, A., and Alleva, E. The 3R principle and the use of non-human primates in the study of neurodegenerative diseases: the case of Parkinson's disease. Neurosci Biobehav Rev **33,** 33, 2009.
32. Shimizu, T., Yamato, M., Isoi, Y., Akutsu, T., Setomaru, T., Abe, K., Kikuchi, A., Umezu, M., and Okano T. Fabrication of

pulsatile cardiac tissue grafts using a novel 3-dimensional cell sheet manipulation technique and temperature-responsive cell culture surfaces. Circ Res **90,** e40, 2002.
33. Shimizu, T., Yamato, M., Kikuchi, A., and Okano, T. Cell sheet engineering for myocardial tissue reconstruction. Biomaterials **24,** 2309, 2003.
34. Harimoto, M., Yamato, M., Hirose, M., Takahashi, C., Isoi, Y., Kikuchi, A., and Okano, T. Novel approach for achieving double-layered cell sheets co-culture: overlaying endothelial cell sheets onto monolayer hepatocytes utilizing temperature-responsive culture dishes. J Biomed Mater Res **62,** 464, 2002.
35. Fissell, W.H. Developments towards an artificial kidney. Expert Rev Med Devices **3,** 155, 2006.

Address correspondence to:
Teruo Okano, Ph.D.
Institute of Advanced Biomedical Engineering and Science
TWIns, Tokyo Women's Medical University
8-1 Kawada-cho, Shinjuku-ku
Tokyo 162-8666
Japan

E-mail: tokano@abmes.twmu.ac.jp

Received: July 6, 2009
Accepted: September 28, 2009
Online Publication Date: November 9, 2009

Reproduced with permission of the copyright owner. Further reproduction prohibited without permission.

A Study of Micro-bubble Enhanced Ultrasound Gene Induction

A. Okamoto[1], R. Tachibana[1], K. Yoshinaka[2], K. Osada[3], S. Takagi[1], K. Kataoka[2,3], U. Chung[2], and Y. Matsumoto[1]

[1] Department of Mechanical Engineering, The University of Tokyo, Tokyo, Japan
[2] Department of Bioengineering, The University of Tokyo, Tokyo, Japan
[3] Department of Materials Engineering, The University of Tokyo, Tokyo, Japan

Abstract— **Recently, a development of the ultrasound gene induction system, called Sonoporation has been investigated. It is known that micro-bubbles can help gene transfection. It is thought that genes are inducted into cells by collapses of cavitation-bubble or micro-bubble. However, the mechanism and optimal induction condition have not been clarified in detail. In this research, we improve gene induction rate by forming DNA/Block copolymer micelle. By forming micelle, DNA is compacted and the stability of DNA is improved. Therefore, it is expected that DNA become able to pass through a hole on cells easily and the expression ability of genes is advanced. Ultrasonic plane wave is exposured from PZT transducer. The frequency is 2MHz and Duty Cycle is 10% (40/360). Mouse fibroblast cell line (NIH3T3) is cultured on the bottom of 24-well plate. We add plasmid DNA and Micro-bubble to culture solution and then exposure ultrasound from above the cells. We use GFP plasmid as reporter gene, and Sonazoid® as micro-bubble. Micelle is formed by combining DNA and block copolymer. Block copolymer is composed of polyethyleneglycol-group and poly-lysine. Each naked DNA and polymer micelle is added to culture medium with microbubble, and then exposure ultrasound. Experimental conditions are set as follows: plasmid density is 15μg/ml, number density of micro-bubble is 1.7×10^5 count/mm^3, ultrasound intensity is 10.2 W/cm^2, ultrasound exposure time is 60 seconds, and sample number is 12. As a result, Gene induction ratio is doubled by forming polymer micelle (from about 1% to about 1.7%). Therefore, the availability of forming polymer micelle is confirmed.**

Keywords— **Ultrasonic therapy, Gene therapy, Gene induction, Buble, Cavitation.**

I. Introduction

Gene therapy is an approach for treating diseases caused by a gene abnormality or deficit. However, gene therapy requires the induction of genes into cells. Various systems to accomplish this have already been devised—for example, viral vectors [1], electroporation [2] and lipofection [3]—but these methods are associated with several problems. Viral vectors have reportedly caused leukemia. Electroporation is not practical for tissues within the body, as the method would require dissection of the affected area and direct application of voltage, while performing gene induction in vitro would require the cells to be delivered to the affected area. Thus, this approach is invasive and would cause patient distress. Lipofection is associated with an unstability of gene. Therefore, an ultrasound gene transfer system, known as sonoporation, has attracted attention. This method allows less invasive and location-specific gene transfection, and it is known that micro-bubbles improve gene transfection rates. Genes are thought to be inducted into cells by the collapse of cavitation bubbles or micro-bubbles [4]. However, the mechanism and optimal induction conditions have not yet been fully clarified. In this research, we examined the availability of forming DNA/Block copolymer micelle. By forming micelle, DNA is compacted and the stability of DNA is improved. Therefore, it is expected that DNA become able to pass through a hole on cells easily and the expression ability of genes is advanced.

II. Materials and Methods

A. Experimental System

Fig.1 shows the experimental apparatus. Mouse fibroblast cell line (NIH3T3) is cultured on the bottom of 24-well plate. We add plasmid DNA and Micro-bubble to culture solution (D-MEM; FBS: 10%; PS: 1%) and then irradiate ultrasonic plane wave from above the cells. We use GFP plasmid as reporter gene, and Sonazoid® as micro-bubble.

Ultrasonic plane wave is emitted from the piezoceramic transducer (PZT) by impressing the amplified sinusoidal signal from the function generator (NF, WF1944A). We use E&I, 2100L as an amplifier. This piezoceramic is flat disk shape and the diameter is 12mm. The direction between the surface of transducer and the bottom of 24-well plate is 3.0mm. The frequency of the signal is 2.0MHz, which is the resonant frequency of Sonazoid®. For limiting damage to cells, we irradiate burst wave ultrasound, whose Duty Cycle is 10% (40/360). Reflected wave is blocked by putting 24-well plate on the water bath and setting acoustic absorbent material under it.

C.T. Lim and J.C.H. Goh (Eds.): WCB 2010, IFMBE Proceedings 31, pp. 1117 1120, 2010.
www.springerlink.com

B. *Ultrasound Intensity*

For the sake of computing the intensity of ultrasound, measurement of sound pressure is done. The transducer is sunk in deggased water and we measure the sound pressure 3.0mm under the surface of piezoceramic with needle hydrophone (production of imotec Messtechnik co. Type 80-0.5-4.0). This measurement is one-dimensional, because the sound pressure distribution made by a flat disk piezoceramic can be thought concentric. Therefore, the axis of measurement is set to pass through the center of piezoceamic. The measurement range is 16mm, which is the diameter of the one well of 24-well plate. The intensity of ultrasound is calculated based on this sound pressure measurement.

C. *Polyplex Micelle*

Micelle is formed by combining DNA and block copolymer (Fig.2). Block copolymer is composed of polyethyleneglycol-group and poly-lysine. In solution, lysine is positive charge, and plasmid DNA is negative charge. Therefore, poly-lysine and DNA interact with each other electrically, and block copolymer and DNA form polymer micelle (Fig.3) [5]. By forming polymer micelle, DNA is compacted [6] and the stability of DNA is improved [7].

Figuration of polymer micelle is controlled by N/P ratio, which is the ratio of amount of positive charge to amount of negative charge. When N/P ratio is high, polymer micelle is small and stability is high, but gene expression is low [8]. In this study, we adopt troid-shaped polymer micelle, which means N/P ratio is 1.5. The size of this polymer micelle is about 300nm.

D. *Confirming the Stability of DNA by Electrocataphoresis*

Naked DNA is attacked by nucleolytic enzyme in serum-containing medium [7] and loses ability of expressing, but this attack can be blocked by forming polymer micelle. Here, we confirm this stability improvement by gel electrocataphoresis.

Plasmid DNA in solution has supercoil (SC) structure. However, if DNA is attacked by nucleolytic enzyme and suffers a loss in at least one of bases, this structure collapses and plasmid DNA has an open circular (OC) structure. These two types of DNA, supercoil and open circular, can be separated by electrophoresis. Each naked DNA and polymer micelle is added to culture medium solution we use in ultrasound exposure experiment. After 15, 30, 60 minutes DNA is cataphoresed. Fig.4 shows the result. SC is the set of plasmids which have supercoil structure. These plasmids are not attacked by enzyme. OC is the one of plasmids which have open circular structure. These are attacked in at least one of bases. Fig.4 shows that most of Naked DNA is attacked by enzyme in 15 minutes. On the other hand, some polymer micelle DNA is immune to this attack for 60 minutes. This means improvement of stability of DNA is realized by forming polymer micelle.

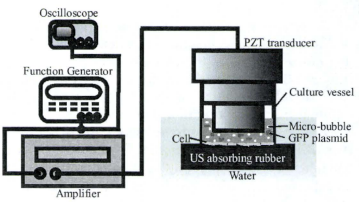

Fig. 1 Experimental apparatus

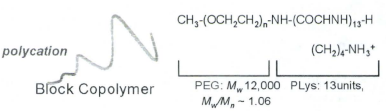

Fig. 2 Block copolymer and its structural fomula [5]

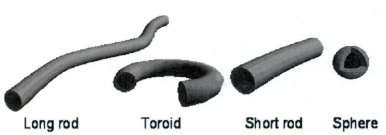

Fig. 3 Polymer micelle [5]

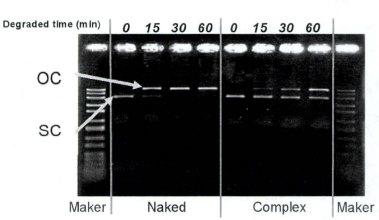

Fig. 4 Electrophoresis

III. Results and Discussions

Each naked DNA and polymer micelle is added to culture medium with micro-bubble, and then we irradiate ultrasound. Experimental conditions are set as follows: plasmid density is 15μg/ml, number density of micro-bubble is 1.7×10^5 count/mm^3, ultrasound intensity is 5.08 W/cm^2, ultrasound exposure time is 60 seconds, and sample number is 12. Gene induction ratio is measured with flow cytometry in 48 hours after ultrasound exposure, since GFP plasmid expression achieves a peak in 48 hours after plasmids induction. Result (Fig.5) shows that gene induction ratio is doubled by forming polymer micelle. Therefore, the availability of forming polymer micelle is confirmed.

This result shows that gene induction ratio is doubled by forming polymer micelle. Forming polymer micelle has two availabilities. First, the size of DNA can be compacted. Normally, plasmid DNA in solution has supercoil structure or open circular structure in solution. Plasmid DNA we use in experiment is composed of about 6000 base pairs (that means the circle of this plasmid is about 2μm), so the size of plasmid DNA is up to 1μm if DNA is expandes absolutely. On the other hand, polymer micelle DNA is, in our study, about 300nm. Therefore, it can be considered that polymer micelle DNA can pass through the hole on cells more easily than naked DNA.

Second, the stability of DNA is improved. Naked DNA is attacked by nucleolytic enzyme in serum-containing medium. In our experimental system we use serum-containing medium when ultrasound is emitted to cells. Therefore, by forming polyplex micelle, the attack by enzyme can be blocked, and the amount of DNA which has the ability of expressing is advanced. We confirm this effect, that is, the blocking of enzyme attack enhanced gene induction ratio, by gene induction experiment without serum.

Naked DNA is added to culture medium with micro-bubble, and then exposure ultrasound. Medium of one sample contains 10% of FBS and 1% of penicillin, while that of the other does not contains FBS and penicillin. After ultrasound exposure, these medium is eliminated and culture medium which contains FBS (10%) and penicillin (1%) is added. This is because cells cannot live for 48 hours without FBS and penicillin. Experimental conditions are set as follows: plasmid density is 15μg/ml, number density of micro-bubble is 1.7×10^5 count/mm^3, ultrasound intensity is 5.08 W/cm^2, ultrasound exposure time is 60 seconds, and sample number is 12. Gene induction ratio is measured 48 hours after ultrasound exposure.

Fig.6 shows the result. It is clear that under serum free condition gene induction ratio is higher than that of with serum medium. Therefore, it can be said that the attack of nucleolytic enzyme diminishes gene induction efficiency and blocking this attack by forming polymer micelle is effective.

The one availability of polymer micelle, that is, the stability enhancement, is demonstrated to be effective to sonoporation. The other availability, compacting the size of DNA, must be demonstrated to be effective by some experiment. However, such kind of experiment has yet to be done.

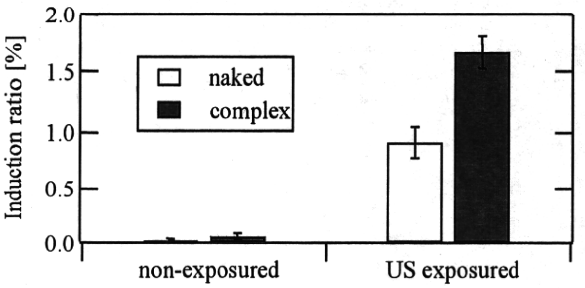

Fig. 5 Gene induction ratio by Naked DNA and polymer micelle

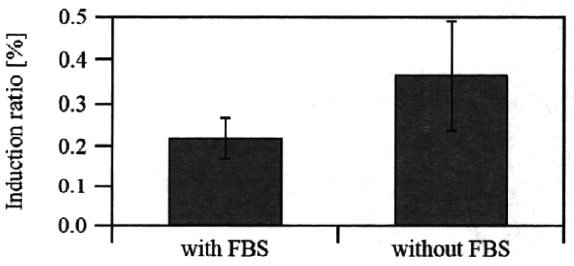

Fig. 6 Gene induction ratio with and without FBS

IV. Conclusion

By forming polymer micelle, stability of DNA in culture medium is improved. This was confirmed by electrocataphoresis. Then we proved that gene induction ratio is doubled by forming polymer micelle. This shows that polymer micelle is available.

Acknowledgment

This work was partially supported by a grant for the Center for NanoBio Integration (CNBI) and Translational Systems Biology and Medicine Initiative (TSBMI), from the Ministry of Education, Culture, Sports, Science and Technology of Japan.

REFERENCES

1. Alexander P, Inder M. V et al. (2001) GENE THERAPY: Promises and Prob-lems. Annu. Rev. Genomics Hum. Genet 2:177-211
2. Weaver J. C, Chizmadzhev, Y. A(1996) Theory of electroporation: A review. Bioelectrochemistry and Bioenergetics 41:135-160
3. Audouy S, Hoekstra D (2001) Cationic lipid-mediated transfection in vitro and in vivo. Molecular Membrane Biology 18:129-143
4. Okada K et al. (2005) A basic study on sonoporation with microbubbles exposed to pulsed ultrasound. J. Med Ultrasonics 32:3-11
5. Itaka K et al.(2009) Recent development of nonviral gene delivery systems with virus-like structures and mechanisms. European Journal of Pharmaceutics and Biopharmaceutics 71:475-483
6. Katayose S, Kataoka K (1997) Water-Soluble polyion complex associates of DNA and poly(ethylene glycol)-poly(L-lysine) block copolymer. Bioconjugate Chem 8:702-707
7. Katayose S, Kataoka K (1998) Remarkable increase in nuclease resistance of plasmid DNA through supermolecular Assembly with poly(ethylene glycol)-poly(L-lysine) block copolymer. Journal of Phamaceutical Science 87-2:160-163
8. M Harada-Shiba et al. (2002) Polyion complex micelles as vectors in gene therapy-pharmacokinetics and in vivo gene transfer. Gene Ther 6:407-414

Author: Akio Okamoto
Institute: The University of Tokyo
Street: 7-3-1, Hongo, Bunkyo ward
City: Tokyo
Country: Japan
Email: a-okamoto@fel.t.u-tokyo.ac.jp

マイクロバブルを援用した超音波遺伝子導入法の高効率化

Efficiency Improvement of Microbubble-Enhanced Sonoporation

○岡本 旭生(東大院)　橘 理恵(東大院)　葭仲 潔 (東大工)　長田 健介 (東大工)　高木 周 (東大工)
片岡 一則 (東大工)　鄭 雄一 (東大工)　松本 洋一郎 (東大工)

AkioOkamoto, Department of Mechanical Engineering, The University of Tokyo, 7-3-1, Hongo, Bunkyo ward, Tokyo, Japan
Rie Tachibana, Department of Mechanical Engineering, The University of Tokyo, 7-3-1, Hongo, Bunkyo ward, Tokyo, Japan
Kiyoshi Yoshinaka, Department of Bioengineering, The University of Tokyo, 7-3-1, Hongo, Bunkyo ward, Tokyo, Japan
Kensuke Osada, Department of Materials Engineering, The University of Tokyo, 7-3-1, Hongo, Bunkyo ward, Tokyo, Japan
Shu Takagi, Department of Mechanical Engineering, The University of Tokyo, 7-3-1, Hongo, Bunkyo ward, Tokyo, Japan
Kazunori Kataoka, Department of Bioengineering, The University of Tokyo, 7-3-1, Hongo, Bunkyo ward, Tokyo, Japan
Chung Ung-il, Department of Bioengineering, The University of Tokyo, 7-3-1, Hongo, Bunkyo ward, Tokyo, Japan
Yoichiro Matsumoto, Department of Mechanical Engineering, The University of Tokyo, 7-3-1, Hongo, Bunkyo ward, Tokyo, Japan

Sonoporation is a recently developed system for gene induction that uses ultrasound. Micro-bubbles are known to aid gene transfection through the introduction of genes into cells by the collapse of cavitation-bubbles (or micro-bubbles). However, the underlying mechanism and optimal introduction conditions have not been clarified in detail. In this research, we improved the gene introduction rate by optimizing burst waveshape of ultrasound and forming DNA/Block copolymer micelles. Micelle formation compacts the DNA and enhances its stability, thereby facilitating the passage of greater amounts of DNA through holes in the cell surface and improving gene expression. Our results show that gene induction ratio is enhanced as the exposed time per pulse and non-exposed time per pulse increase. The gene induction ratio is doubled by the formation of polymer micelles (from ~1% to ~2%), thereby confirming that the system is capable of generating polymer micelles for introducing DNA into cells.

Key Words:　Cavitation, Gene therapy, Cellular membrane, Bubble, Polymer micelle

1. はじめに

遺伝子治療とは，異常遺伝子を持つ細胞に対して新たに遺伝子を導入し，細胞の機能を正常化することで病気を治療する方法である．現在までに確立されている遺伝子導入法は侵襲性，副作用の危険性といった問題点を抱えており，低侵襲かつ副作用のない超音波遺伝子導入法が着目されている．超音波遺伝子導入法は超音波照射により細胞膜に一時的な小孔を物理的に生じさせることで遺伝子導入を実現する手法であり，マイクロバブルの援用により導入の効率が向上するという知見がある[1]．マイクロバブル援用超音波遺伝子導入法では超音波照射により生じるマイクロバブルの振動，崩壊といった現象を用いて細胞膜に小孔を一時的に生じさせ，遺伝子導入を実現していると考えられているが，[2]詳細な機序は不明である．また，遺伝子導入効率が他手法に比べ低いという問題がある．

超音波遺伝子導入法における細胞への小孔形成を評価した先行研究より，全細胞の 60%程度に小孔が形成される条件においても遺伝子導入率は 0.1%程度であることが示されている[3]．本研究は小孔形成細胞に対し効率的に遺伝子を導入する手法の開発を目的とし，超音波照射条件を最適化し，マイクロバブルの細胞に対する寄与を増大させる．また，遺伝子の高分子ミセル化によりサイズを縮小し安定性を向上させた上で超音波照射実験を行う．

2. 遺伝子導入実験システム

2-1 実験装置　超音波遺伝子導入実験装置の概略図を Fig.1 に示す．マウス性線維芽細胞系 NIH3T3 を細胞培養容器に培養する．細胞培養液として D-MEM (Dulbecco's Modified Eagle Medium) に，血清である FBS を 10%，抗生物質である PS (penicillin-streptomycin) を 1%加えたものを用いる．ウェル内の細胞培養液に導入遺伝子とマイクロバブルを混和し，平面超音波を上方より照射する．導入遺伝子は緑色蛍光蛋白質(GFP)プラスミドを，マイクロバブルは Sonazoid® を用いる．平面超音波は直径 12 mm の円盤状のピエゾトランスデューサにファンクションジェネレータで発生させた信号をアンプで増幅し入力することで照射する．超音波の周波数は Sonazoid® の共振周波数である 2.0 MHz とし，細胞培養容器より 3 mm 上方より照射する．細胞へのダメージを抑制するため照射超音波の波形をバースト波形とする．水槽内にて細胞培養容器を吸音材の上に設置することで超音波の反射を防ぐ．遺伝子濃度を 15 μg/ml，マイクロバブル数密度を 1.7×10^5 /mm^3，サンプル数を 12 とする．

2-2 遺伝子導入率測定　GFP プラスミドが導入された細胞は細胞内で緑色蛍光タンパク質(GFP)を生成するため，遺伝子が導入された細胞が判別可能となる(Fig.2)．細胞内における GFP の生成量は遺伝子導入後 48 時間後にピークに達する為，超音波照射から 48 時間後にフローサイトメトリにより遺伝子導入率を測定する．フローサイトメータの細い流路に細胞を一個ずつ流し，レーザー光をあて，その散乱光により流路を流れた全

細胞数，および遺伝子導入細胞数を測定する．全細胞に対する遺伝子導入細胞の割合を遺伝子導入率と定義する．

2-3 細胞生存率測定法 本手法の細胞への毒性を評価するため，細胞の生存率を細胞毒性試験試薬 Cell Counting Kit 8 (以下 CCK8)を用いて測定する．CCK8 は生細胞の代謝により還元され，橙色の formazan が生成される．formazan 生成量は生細胞数に比例し，溶液中の formazan 量と溶液の吸光度も比例する．したがって，CCK8 を加えた細胞培養液の吸光度からサンプルの生存率を求めることができる．超音波照射を行わない細胞の培養液に formazan を加えたものをコントロールとし，コントロールの吸光度とサンプル培養溶液の 450 nm の吸光度を比較することで生存率を求める．遺伝子導入率と同じく超音波照射から 48 時間後に細胞培養液に CCK8 を加え，3 時間程度呈色反応させた後，吸光度を測定する．

3. バースト波形をパラメータとした遺伝子導入実験

3-1 バースト波形依存性測定実験 超音波の波形をバーストとすることで，Fig.3 のように一定の照射時間に対し照射休み時間を設けることになり，連続波に比べ細胞へのダメージが抑制されるという知見が得られている[4]．本研究ではこのバースト波形に着目し，遺伝子導入率のバースト波形に対する依存性を調査する．1 パルスにおける照射時間，照射休み時間，および単位時間におけるパルス数である PRF をバースト波形のパラメータとし，それぞれに対する遺伝子導入率の依存性を 2 章に記した方法で測定する．ただし，1 パルス当たりの照射時間，照射休み時間の単位を cycle とする．本研究では 2.0 MHz の超音波を用いるため，1cycle は 0.5 μs に相当する．

まず 1 パルスにおける照射時間に対する依存性を調べるため，照射休み時間を 100 cycle と固定し，照射時間を 10, 100, 1000 cycle と変化させたときの遺伝子導入率を測定する．照射時間に応じて全照射時間を変化させ，全照射時間における投入エネルギー量を固定する．照射時間 10 cycle のサンプルに対し全照射時間を 110 s, 100 cycle のものに対し 20 s, 1000 cycle としたものに対し 11 s とする．照射休み時間に対する依存性についても同様に，照射時間を 100 cycle と固定し，照射休み時間を 10, 100, 1000 cycle と変化させる．全照射時間は，照射休み時間 10 cycle のサンプルに対し 11 s, 100 cycle のものに対し 20 s, 1000 cycle のものに対し 110 s とする．また，照射時間と照射休み時間の比である Duty 比を 10%と固定したときの，PRF に対する依存性を測定する．PRF を 50, 500, 5000, 50000 Hz と変化させ，全照射時間を 60 s とする．以上の実験において超音波強度を 5.0 W/cm^2 とする．

3-2 結果と考察 Fig.4 (a),(b)は照射時間をパラメータとした実験の結果である．これより，照射時間が長いほど，遺伝子導入率が向上し，生存率は低下していることが判る．これは，照射時間の増大に伴い 1 パルス間に生じる細胞膜表面の小孔のサイズが大きくなることに起因すると考察される．

Fig.5 (a),(b)は照射休み時間をパラメータとした実験の結果を示している．照射休み時間の増加に伴い，遺伝子導入率，細胞生存率ともに向上していることがわかる．これは，十分な照射休み時間を設けることで細胞へのダメージが抑制されたため，小孔が生じ遺伝子が導入された細胞が生存できるようになったことに起因すると考察される．

Fig.6 (a),(b)はPRFをパラメータとした結果である．PRFが小さいほど遺伝子導入率が高いことがわかる．PRF が低いほど照射時間，照射休み時間ともに長くなるため，この結果は照射時間，および照射休み時間依存性と一致するといえる．また，PRF が小さいほど細胞生存率は低下していることがわかる．これは，低 PRF で照射時間が長くなり，細胞へのダメージが大きくなるためと予想される．

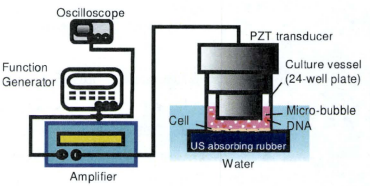

Fig.1 Experimental apparatus

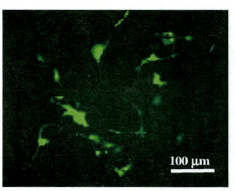

Fig.2 Fluorescent observation of GFP

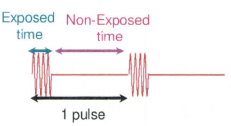

Fig.3 Burst waveshape

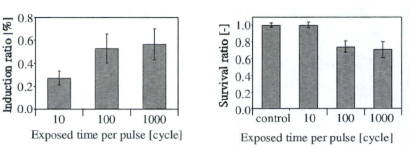

Fig.4 Dependency on exposed time per pulse

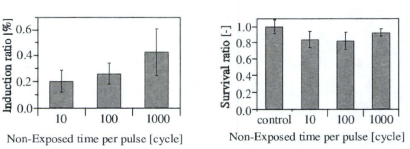

Fig.5 Dependency on Non-Exposed time per pulse

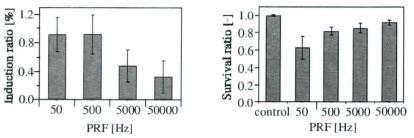

Fig.6 Dependency on PRF

4. プラスミドの高分子ミセル化

4-1 高分子ミセル 遺伝子の高分子ミセル化にはブロック共重合体(Fig.7)を用いる. ブロック共重合体はポリエチレングリコール基の先端にリジンが 13 個結合したものである. プラスミドは溶液中で負に帯電しているのに対し, リジンは正に帯電している. そのため, プラスミドはブロック共重合体中のリジンと電気的に相互作用し, 溶液中で高分子ミセル(Fig.8)を形成する[5].

細胞培養液中の核酸分解酵素が機能するとプラスミドの塩基配列が損なわれる. タンパク質発現に必要となる塩基が損なわれるとプラスミドは発現性を失う. 高分子ミセル化されたプラスミドは核酸分解酵素の影響を受けにくくなるため, 培養液中での安定性が向上する[6]. また, 高分子ミセル化によりプラスミドのサイズが縮小される[6]. そのため, 超音波照射により生じた細胞表面の小孔を通過しやすくなることが期待される.

高分子ミセルの形状, 性質を制御するパラメータとして N/P 比を用いる. N/P 比は, プラスミドの持つ負電荷の総量に対する, ブロック共重合体の持つ正電荷の総量の比と定義される. N/P 比が大きいほど高分子ミセルは小さくなり, 同時に安定性も向上するが, 発現性は低下する[7]. 本研究では N/P 比を 1.5 とする. N/P 比が 1.5 の状態では高分子ミセルはドーナツ型となり, このときのサイズは 300nm 程度である. 本研究で用いるプラスミドはおよそ 6000 の塩基対より構成され, 最大で 1 μm 程度の広がりを持つため, 高分子ミセル化によりサイズ縮小が実現されているといえる.

4-2 電気泳動による遺伝子の安定性の確認 前述した高分子ミセル化によるプラスミドの安定性向上の効果をゲル電気泳動により評価する. プラスミドは溶液中でスーパーコイルと呼ばれる高次構造をとるが, 核酸分解酵素の機能で塩基が損なわれることによりオープンサーキュラーやリニアへと高次構造が変化する[8]. 異なる高次構造のプラスミドは電気泳動で分離できるため, 高次構造の時間変化を可視化することで核酸分解酵素存在下でのプラスミドの安定性を評価することができる.

通常のプラスミドまたは高分子ミセル化プラスミドを細胞培養溶液に加え, 一定時間反応させた後, EDTA,DDTA を溶液に加えミセルを解離させ, 電気泳動を行う. 反応時間は 0, 15, 30, 60 分とし, プラスミド濃度は遺伝子導入実験と等しく 15 μg/ml とする. 電気泳動の結果を Fig.9 に示す. 図中の SC はスーパーコイル, OC はオープンサーキュラーの高次構造をとるプラスミドである. 通常のプラスミドは 15 分以内にほぼすべてがオープンサーキュラーに変化しているのに対し, 高分子ミセル化したものはこの変化が抑制されていることが分かる. これはプラスミドの高分子ミセル化により細胞培養液中での安定性が向上していることを示している.

4-3 高分子ミセル化プラスミド導入実験 通常のプラスミド, または高分子ミセル化したプラスミドを細胞に導入する実験を行う. 実験は 2 章に記した方法で行い, 超音波強度を 5.1 W/cm^{2}とする. 結果を Fig.10 に示す. 遺伝子の高分子ミセル化により, 遺伝子導入率が向上していることがわかる. これはプラスミドの高分子ミセル化により超音波遺伝子導入法の高効率化が可能であることを示している.

4-4 血清のない状態での遺伝子導入実験 前述したとおり, DNA の高分子ミセル化により, DNA は細胞培養液中に存在する核酸分解酵素の影響を受けにくくなり, 安定化する. 本実験系における核酸分解酵素の影響を, 血清のない状態で Naked の遺伝子を導入する実験を行うことで評価する.

24 ウェルプレートに細胞を培養し, 培養液を吸引除去し, FBS を 10%, PS を 1%含む D-MEM を加えたもの, 及び両者を含まない D-MEM を加えたものを用意する. これらのサンプルに対し 2 章に記した方法で Naked の DNA を導入する実験を行う. 超音波強度を 5.1 W/cm^{2}とする. 実験結果 (Fig.11) より, 血清を含む培養液を用いると遺伝子導入率が低下していることがわかる. これは, 核酸分解酵素の機能により遺伝子導入が妨げられていることを示している. DNA を高分子ミセル化することで核酸分解酵素の機能を制限することが, 遺伝子導入率の向上に寄与したと考えられる.

高分子ミセル化によるメリットの 1 つである遺伝子の安定化が遺伝子導入率向上に寄与していることを本実験で検証した. しかし, もう1つのメリットであるサイズ縮小が遺伝子導入率向上に寄与していることは検証されていないため, 粒子導入実験などにより検証する必要がある.

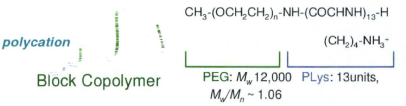

Fig.7 Block copolymer and its structural fomula [5]

Fig.8 Polyplex micelle [5]

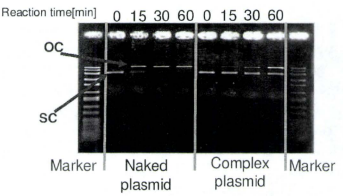

Fig.9 Electrophoresis

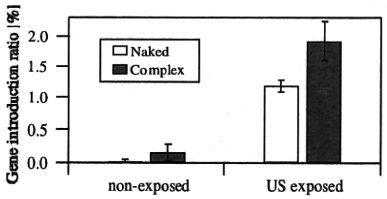

Fig.10 Gene introduction ratio by Naked DNA and micelle

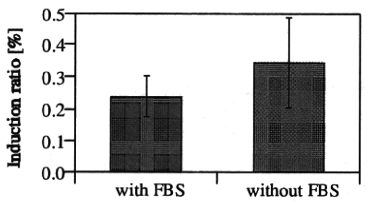

Fig.11 Gene induction ratio with and without FBS

5. 結論

本研究ではマイクロバブルを援用した超音波遺伝子導入法の高効率化を目指し，以下の知見を得た．

超音波のバースト波形をパラメータとした遺伝子導入実験より，1 パルスにおける照射時間が長いほど，照射休み時間が長いほど遺伝子導入効率が向上することを示した．PRF をパラメータとした実験では低 PRF で遺伝子導入率が高くなることが示され，照射時間，照射休み時間依存性と一致した．

DNA のサイズ縮小，および安定化により遺伝子導入効率が向上することを，高分子ミセル化 DNA 導入実験により示した．

謝辞

本研究の一部は、ナノバイオ・インテグレーション研究拠点(CNBI)，システム疾患生命科学による先端医療技術開発拠点 (TSBMI)の支援を受けて実施したものである．ここに記して謝意を表する．

参考文献

[1] Hirayama K et al., Proc. of 6th ISTU, 2006
[2] Okada K et al., "A Basic Study on Sonoporation with Microbubbles Exposed to Pulsed Ultrasound," J. Med Ultrasonis, Vol. 32, pp. 3-11, 2005.
[3] Tachibana R et al., Proc of 9th ISTU, 2009
[4] Hun P et al, Study of Sonoporation Dynamics Affected by Ultrasound Duty Cycle", Ultrasound Med Bio, Vol. 31, pp. 849-856
[5] Itaka K et al., "Recent Development of Nonviral Gene Delivery Systems with Virus-like Structures and Mechanisms," European Journal of Pharmaceutics and Biopharmaceutics, Vol. 71, pp. 475-483, 2009.
[6] Katayose S et al., "Remarkable Increase in Nuclease Resistance of Plasmid DNA through Supermolecular Assembly with Poly(ethylene glycol)-poly(L-lysine) Block Copolymer," Journal of Phamaceutical Science, Vol.87-2, pp. 160-163, 1998.
[7] M Harada-Shiba et al., "Polyion Complex Micelles as Vectors in Gene Therapy-pharmacokinetics and in vivo Gene Transfer," Gene Ther. Vol.6, pp. 407-414, 2002.
[8] Benjamin Lewin, "遺伝子(上)," 東京化学同人